JOC Article

Understanding the Participation of Quadricyclane as Nucleophile in Polar [2σ + 2σ + 2π] Cycloadditions toward Electrophilic π Molecules

Luis R. Domingo,* José A. Saéz, Ramón J. Zaragozá, and Manuel Arnó

Departamento de Química Orgánica, Universidad de Valencia, Dr. Moliner 50, E-46100 Burjassot, Valencia, Spain

domingo@utopia.uv.es

Received July 16, 2008

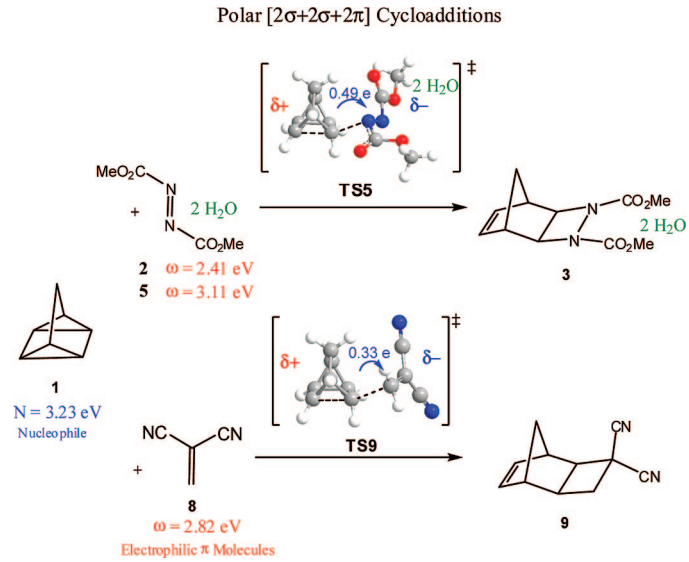

The formal [2σ + 2σ + 2π] cycloaddition of quadricyclane, **1**, with dimethyl azodicarboxylate, **2**, in water has been studied using DFT methods at the B3LYP/6−31G** and MPWB1K/6−31G** levels. In the gas phase, the reaction of **1** with **2** has a two-stage mechanism with a large polar character and an activation barrier of 23.2 kcal/mol. Inclusion of water through a combined discrete-continuum model changes the mechanism to a two-step model where the first nucleophilic attack of **1** to **2** is the rate-limiting step with an activation barrier of 14.7 kcal/mol. Analysis of the electronic structure of the transition state structures points out the large zwitterionic character of these species. A DFT analysis of the global electrophilicity and nucleophilicity of the reagents provides a sound explanation about the participation of **1** as a nucleophile in these cycloadditions. This behavior is reinforced by a further study of the reaction of **1** with 1,1-dicyanoethylene.

Introduction

Cycloaddition reactions are one of the most important processes with both synthetic and mechanistic interest in organic chemistry[1] In general, in this type of reaction, two new σ bonds are formed at the ends of two interacting π systems along with the formation of a carbocyclic system. In some cases, a part of the π system involved in the cycloaddition is replaced by a strained σ system, thus allowing these σ bonds to participate in the cycloaddition process. Highly polar transition states have not been postulated for cycloadditions because the rates of the reactions are often insensitive to solvent polarity.[2] However,

* Corresponding author. Tel: 34 96 3543106; Fax: 34 96 3544328.

(1) (a) Carruthers, W. *Some Modern Methods of Organic Synthesis*, 2nd ed.; Cambridge University Press: Cambridge, 1978. (b) Carruthers, W. *Cycloaddition Reactions in Organic Synthesis*; Pergamon: Oxford, 1990.

(2) Carey, F. A.; Sundberg, R. J. *Advanced Organic Chemistry. Part A. Structure and Mechanisms*, 4th ed.; Plenum: New York, 2000.

10.1021/jo801575g CCC: $40.75 © 2008 American Chemical Society
Published on Web 10/23/2008

certain Diels−Alder (DA) reactions of hydrophobic compounds have been found to be accelerated in dilute aqueous medium.[3]

In recent years, Sharpless[4] has focused on the modular synthetic techniques that rely on the few nearly perfect reaction types. In the course of his work, he noticed that many such reactions often proceed optimally in pure water.[5] In connection with his studies, Sharpless recently explored the preparation of 1,2-diazetidines from quadricyclane (QDC, **1**), through a [2σ + 2σ + 2π] cycloaddition with dimethyl azodicarboxylate (DMAD, **2**),[6] discovered by Lemal and co-worker (see Scheme 1).[7] The typical reaction conditions involve heating **1** with **2** in toluene or benzene at 80 °C for 24 h or longer. In contrast, when a mixture of **1** and **2** was vigorously stirred "on water" the heterogeneous reaction was completed within a few minutes at ambient temperature (see Scheme 1).[6] When the reaction was carried out under homogeneous conditions, polar protic solvents accelerate the reaction, suggesting that hydrogen bonds (HB), charge stabilization, and dipolar effects may be important for rate acceleration.[8] It is worth noting that when the cycloaddition was carried out in water under homogeneous conditions (a 3:1 methanol/H_2O mixture, 4 h), the reaction proceed slower than under heterogeneous conditions "on water", but it was faster than the homogeneous reaction in methanol (18 h), suggesting that the water molecules play a relevant role in these solvent-catalyzed cycloadditions.

SCHEME 1

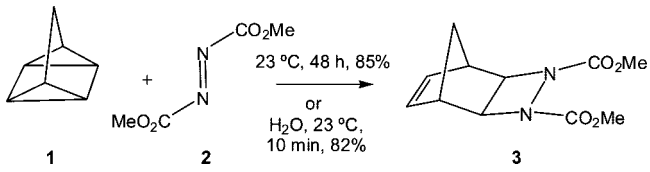

The decrease of the activation barrier in the cycloaddition reactions has been associated to the zwitterionic character of the transition state structures (TSs) involved in such processes, that is, the polar character of the cycloaddition.[9,10] In this way, the characterization of the electrophilic/nucleophilic nature of reagents allows prediction of the polar character of the cycloaddition and, as a consequence, the feasibility of the entire process. Formal [2 + 2], [4 + 2], [3 + 2], and [3 + 4] cycloaddition reactions have been shown to obey this rationalization.[10b] For instance, Lewis acid-catalyzed cycloadditions take place through TSs with a large zwitterionic character.[11] Recent studies have shown that formation of nonclassical,[12] C═O···H−C, and classical,[13] C═O···H−O, HBs to carbonyl compounds accelerate the DA reactions as they become a more polar process. This acceleration can be associated to the increase in electrophilicity of the carbonyl compound that is hydrogen bonded, as in Lewis acid catalysis, increasing the polarity of the process.[12a]

The thermal uncatalyzed [2σ + 2σ + 2π] cycloadditions of **1** with alkenes and alkynes have been assumed to follow a concerted mechanism.[14] The most convincing experimental evidence for a concerted mechanism comes from stereochemical studies which found that the reaction of **1** with *cis* and *trans* alkenes gave products which preserved the original alkene stereochemistry. However, this observation does not discard a nonconcerted pathway, which proceeds via a biradical intermediate, where the formation of the cycloadduct is faster than the rotation in the biradical. In order to understand the mechanism of these thermal cycloadditions, Houk, Carpenter, and co-workers[15] performed a UB3LYP/6−31G* study of the [2σ + 2σ + 2π] cycloaddition of **1** with ethylene, acetylene, dicyanoacetylene, and dimethyl acetylenedicarboxylate (DMAcD). For these reactions, nonconcerted pathways, which proceed via biradical intermediates, were found (see Scheme 2). For the reaction between **1** and ethylene, the activation barrier associated to the formation of the biradical intermediate **BR1** via **TS1** was 35.2 kcal/mol, a larger value than that computed for the cycloaddition of **1** to DMAcD, 21.5 kcal/mol.[15] The large acceleration found at the reaction of **1** with DMAcD can be related to the high electrophilic character of this acetylene derivative, which promotes polar cycloadditions toward nucleophilic species.[16]

SCHEME 2

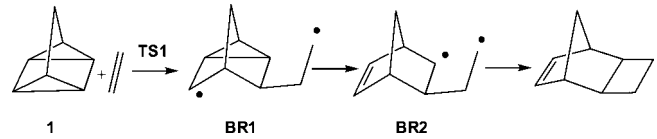

Protic solvent effects on DA reactions by HB formation have been widely studied. In an early work, Blake et al.[17] studied the effects of the HB involving water molecules on the DA TSs. They found a more favorable HB interaction (between 1.5 and 2.0 kcal/mol at HF/6−31G*) for the TS with a HB over the oxygen atom with respect to the ground state. Evanseck et al.[18] studied the rate acceleration and the *endo/exo* selectivity of the butadiene and acrolein DA reaction in aqueous phase using B3LYP/6−31G* calculations. The experimental acceleration and the enhanced *endo/exo* selectivity were reproduced only when solvation forces were approximated by a discrete-continuum model, obtaining activation energies that were in excellent agreement with the experiments. Jorgensen et al.[19] used

(3) (a) Breslow, R. *Acc. Chem. Res.* **1991**, *24*, 159–164. (b) Breslow, R. *ACS Symp. Ser.* **1994**, *568*, p 291.
(4) Kolb, H. C.; Finn, M. G.; Sharpless, K. B. *Angew. Chem.* **2001**, *113*, 2056–2075.
(5) Fokin, V. V.; Sharpless, K. B. *Angew. Chem.* **2001**, *113*, 3563–3565.
(6) Narayan, S.; Muldoon, J.; Finn, M. G.; Fokin, V. V.; Kolb, H. C.; Sharpless, K. B. *Angew. Chem., Int. Ed.* **2005**, *44*, 3275–3279.
(7) Rieber, N.; Alberts, J.; Lipsky, J. A.; Lemal, D. M. *J. Am. Chem. Soc.* **1969**, *91*, 5668–5669.
(8) (a) Rodgman, A.; Wright, G. F. *J. Org. Chem.* **1953**, *18*, 465–484. (b) Gast, L. E.; Bell, E. W.; Teeter, H. M. *J. Am. Oil Chem. Soc.* **1956**, *33*, 278–281.
(9) Domingo, L. R.; Arno, M.; Andres, J. *J. Org. Chem.* **1999**, *64*, 5867–5875.
(10) (a) Domingo, L. R.; Aurell, M. J.; Perez, P.; Contreras, R. *Tetrahedron* **2002**, *58*, 4417–4423. (b) Pérez, P.; Domingo, L. R.; Aizman, A.; Contreras, R. In*Theoretical Aspects of Chemical Reactivity*; Toro-Labbé, A., Ed.; Elsevier Science: New York, 2006; Vol. 19, pp 167−238.
(11) Arnó, M.; Zaragozá, R. J.; Domingo, L. R. *Eur. J. Org. Chem.* **2005**, 3973–3979.
(12) (a) Domingo, L. R.; Andres, J. *J. Org. Chem.* **2003**, *68*, 8662–8668. (b) Polo, V.; Domingo, L. R.; Andres, J. *J. Phys. Chem. A* **2005**, *109*, 10438–10444.
(13) (a) Gordillo, R.; Dudding, T.; Anderson, C. D.; Houk, K. N. *Org. Lett.* **2007**, *9*, 501–503. (b) Anderson, C. D.; Dudding, T.; Gordillo, R.; Houk, K. N. *Org. Lett.* **2008**, 2749–2752.
(14) (a) Paquette, L. A.; Kesselmayer, M. A.; Kunzer, H. *J. Org. Chem.* **1988**, *53*, 5183–5185. (b) Tabushi, I.; Yamamura, K.; Yoshida, Z. *J. Am. Chem. Soc.* **1972**, *94*, 787–792.
(15) Jones, G. A.; Shephard, M. J.; Paddon-Row, M. N.; Beno, B. R.; Houk, K. N.; Redmond, K.; Carpenter, B. K. *J. Am. Chem. Soc.* **1999**, *121*, 4334–4339.
(16) (a) Domingo, L. R.; Picher, M. T.; Zaragoza, R. J. *J. Org. Chem.* **1998**, *63*, 9183–9189. (b) Domingo, L. R.; Arnó, M.; Contreras, R.; Pérez, P. *J. Phys. Chem. A* **2002**, *106*, 952–961.
(17) Blake, J. F.; Lim, D.; Jorgensen, W. L. *J. Org. Chem.* **1994**, *59*, 803–805.
(18) Kong, S.; Evanseck, J. D. *J. Am. Chem. Soc.* **2000**, *122*, 10418–10427.
(19) Chandrasekhar, J.; Shariffskul, S.; Jorgensen, W. L. *J. Phys. Chem. B* **2002**, *106*, 8087–8085.

QM/MM simulations to study the free energy profiles of DA reactions in water. The free activation energy of the cycloaddition between methyl vinyl ketone and butadiene is reduced on going from the gas phase to water in 2.8 kcal/mol. These authors concluded that the rate increase in water arises in part from the hydrophobic association of the reactants but mainly from enhanced hydrogen bonding between water molecules and the polarized TS.

Recently, we reported a density functional theory (DFT) study about the enhanced reactivity of carbonyl compounds on DA reactions via nonclassical HB formation to chloroform.[12] The effects of chloroform were modeled by means of discrete-continuum models. In the gas phase, the formation of specific HBs between acetone and two chloroform molecules decreased the activation barriers from 19.3 to 8.5 kcal/mol (B3LYP/6−31G*). Inclusion of solvent effects through the combination of discrete and polarizable continuum models yielded a change of molecular mechanism from a two-stage[20] to a two-step mechanism where the first step was rate-limiting and had an activation barrier of 9.6 kcal/mol. Similar results have been recently reported by Houk et al. for the alcohol-catalyzed DA reactions of acrolein and benzaldehyde with a nucleophilic Rawal's diene.[13]

Finishing the present study, Jung and Marcus[23] reported a study about the theory of organic catalysis "on water". For this purpose, they performed a (U)B3LYP/6−31+G* study of the [2σ + 2σ + 2π] cycloaddition of **1** with **2** "on water". Two computational models were studied (see Scheme 3): the gas-phase reaction of **1** with **2** as a neat reaction and the reaction of **1** with **2** hydrogen-bonded to three water molecules, **4**, as a surface reaction. While for the neat reaction these authors proposed a stepwise mechanism via a biradical intermediate **BR3** similar to that reported by Houk, Carpenter, and co-workers,[15] for the surface reaction they found a concerted mechanism via **TS4** (see Scheme 3). They indicated that the lowering of the activation barrier by about 7 kcal/mol (22 kcal/mol (**TS2**) versus 15 kcal/mol (**TS4**)) was due to the HB with the free OH groups of water at the interface and, therefore, it was the responsible for the acceleration of "on water" reactions. They suggested that the different extent of HB formation for reactants and TSs was responsible for the barrier reduction and the acceleration of the surface reaction.

SCHEME 3

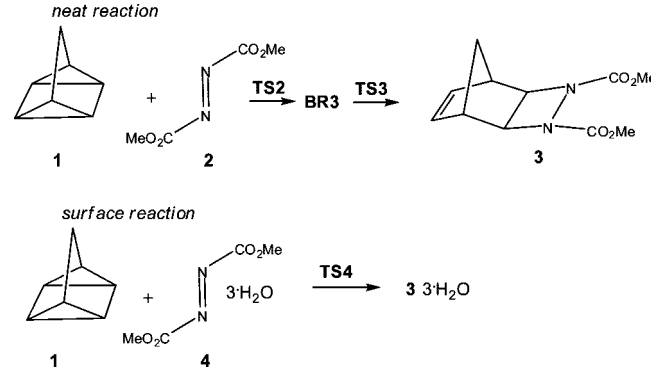

Although the catalytic effects by HB in cycloaddition reactions have been studied, the potential participation of QDC **1**, a strained saturated hydrocarbon, in polar processes encouraged us to perform a theoretical study. Thus, the nucleophilic behavior of **1**, unusual in saturated hydrocarbon chemistry, could open polar reactivity instead of nonpolar reactivity, via biradical species, as in the species proposed by Houk, Carpenter, and co-workers.[15] With this aim, we have performed a DFT study of the formal [2σ + 2σ + 2π] cycloaddition of **1** to **2** in absence and in presence of explicit water molecules (see Schemes 4 and 5). Note that the combined discrete-continuum model used in the present study is a simplified model of the reaction in water. Since the heterogeneous reaction "on water" requires a more complex model, we assume that the electronic effects responsible for the observed acceleration in water are also present in the reaction "on water". The analysis of the reactivity indexes defined within the conceptual DFT will be used to explain the catalytic effects of water solvent molecules found by Sharpless, as well as the participation of **1** as a nucleophile in polar cycloaddition reactions. Finally, the polar cycloadditions of QDC and bicyclo[2.2.1]hepta-2,5-diene, **10**, to 1,1-dicyanoethylene (DCE, **8**), a good electrophilic ethylene,[24] have been studied in order to determine the nucleophilic reactivity of **1** toward electrophilic π molecules (see Scheme 6).

Computational Methods

First, DFT calculations were carried out using the B3LYP[25] exchange-correlation functionals, together with the standard 6−31G** basis set.[26] This methodology has been widely used in the study of HB-catalyzed DA reactions.[12,13,18] Recent DFT studies have indicated that the new exchange-correlation functional (MPWB1K) developed by Zhao and Truhlar performs well for HB and weak interactions without BSSE corrections.[27] So, the B3LYP/6−31G** geometries were subsequently optimized at the MPWB1K/6−31G** level. The optimizations were carried out using the Berny analytical gradient optimization method.[28] A comparison of the geometries and electronic structures of the TSs obtained with the two functionals showed that there are not great differences in the bond formation and bond breaking, but the MPWB1K activation barriers

(20) In an old paper, Dewar defined the two-stage[21a] reactions as "concerted but not synchronous, in which some of the changes in bonding takes place in the first half of the reaction while the rest takes place in the second half". [21b] More recently, Houk proposed that "the two-stage mechanism, in which the formation of the two bonds take place in separate but overlapping processes, would be called an asynchronous concerted process".[21c] Both definitions associate the two-stage reactions to concerted bond-formation processes. However, recent studies carried out in cycloaddition reactions, which take place in a single kinetic step but through highly asynchronous TSs, have indicated that the formation of the two new σ bonds is nonconcerted.[22] Therefore, we propose that the concept of two-stage reactions should be used for those reactions in which formation of the two σ bonds takes place in a nonconcerted process but in a single kinetic step. At the unique high asynchronous TS found in the two-stage reactions, only one σ bond is being formed along a two-center interaction. From this TS, and only when the formation of the first σ bond is very advanced, the formation of the second σ bond begins.[22] However, just at this stage of the reaction, going downward to cycloadduct, the changes in bonding do not have any relevance from a kinetic point of view. Note that at the unique TS of an asynchronous concerted process, the formation of the two σ bonds takes place at the same time but to a different extent.

(21) (a) Goldstein, M. J.; Thayerjr, G. L., Jr. *J. Am. Chem. Soc.* **1965**, *87*, 1933–1941. (b) Dewar, M. J. S.; Olivella, S.; Stewart, J. J. P. *J. Am. Chem. Soc.* **1986**, *108*, 5771–5779. (c) Houk, K. N.; González, J.; Li, Y. *Acc. Chem. Res.* **1995**, *28*, 81–90.

(22) (a) Domingo, L. R. *J. Org. Chem.* **2001**, *66*, 3211–3214. (b) Berski, S.; Andrés, J.; Silvi, B.; Domingo, L. R. *J. Phys. Chem. A* **2006**, *110*, 13939–13947.

(23) Jung, Y.; Marcus, R. A. *J. Am. Chem. Soc.* **2007**, *129*, 5492–5502.

(24) Domingo, L. R.; Chamorro, E.; Pérez, P. *J. Org. Chem.* **2008**, *73*, 4615–4624.

(25) (a) Becke, A. D. *J. Chem. Phys.* **1993**, *98*, 5648–5652. (b) Lee, C.; Yang, W.; Parr, R. G. *Phys. Rev. B* **1988**, *37*, 785–789.

(26) Hehre, W. J.; Radom, L.; Schleyer, P. v. R.; Pople, J. A. *Ab Initio Molecular Orbital Theory*; Wiley: New York, 1986.

(27) Zhao, Y.; Truhlar, G. D. *J. Phys. Chem. A* **2004**, *108*, 6908–6918.

(28) (a) Schlegel, H. B. *J. Comput. Chem.* **1982**, *3*, 214–218. (b) Schlegel, H. B. Geometry Optimization on Potential Energy Surfaces In *Modern Electronic Structure Theory*; Yarkony, D. R., Ed.; World Scientific Publishing: Singapore, 1994.

were in better agreement with the experimental activation energy for the reaction of **1** with **2** in water.[6] Consequently, we will discuss only MPWB1K/6−31G** results, while the B3LYP/6−31G** energies and geometries are given in Supporting Information. The stationary points were characterized by frequency calculations in order to verify that TSs have one and only one imaginary frequency. The intrinsic reaction coordinate (IRC)[29] paths were traced in order to check the energy profiles connecting each TS to the two associated minima of the proposed mechanism using the second-order González−Schlegel integration method.[30] The values of the MPWB1K enthalpies, entropies, and free energies were calculated with the standard statistical thermodynamics at 298.15 K.[26] Thermodynamic calculations were scaled by a factor of 0.96. The electronic structures of stationary points were analyzed by the NBO method.[31] All calculations were carried out with the Gaussian 03 suite of programs.[32]

Solvent effects have been considered at the same level of theory by geometry optimization of the gas-phase structures using a self-consistent reaction field (SCRF)[33] based on the polarizable continuum model (PCM) of the Tomasi's group.[34] Since this cycloaddition was carried out in water, we selected its dielectric constant at 298.0 K, $\varepsilon = 78.39$.

The global electrophilicity index,[35] ω, which measures the stabilization energy when the system acquires an additional electronic charge ΔN from the environment, has been given by the following simple expression,[35] $\omega = (\mu^2/2\eta)$, in terms of the electronic chemical potential μ and the chemical hardness η. Both quantities may be approached in terms of the one-electron energies of the frontier molecular orbitals HOMO and LUMO, ε_H and ε_L, as $\mu \approx (\varepsilon_H + \varepsilon_L)/2$ and $\eta \approx (\varepsilon_L - \varepsilon_H)$, respectively.[36] Recently, we introduced an empirical (relative) nucleophilicity index, N, based on the HOMO energies obtained within the Kohn−Sham scheme,[37] and defined as $N = E_{HOMO(Nu)} - E_{HOMO(TCE)}$.[24] The nucleophilicity is referred to tetracyanoethylene (TCE) taken as a reference, because it presents the lowest HOMO energy in a large series of molecules already investigated in the context of polar cycloadditions. This choice allows us to conveniently handle a nucleophilicity scale of positive values.[24] The reactivity indices were computed from the B3LYP/6−31G* HOMO and LUMO energies at the ground-state of the molecules.

For the present study, three reaction models have been selected (see Scheme 4, 5 and 6): reaction Model I corresponds to the gas-phase $[2\sigma + 2\sigma + 2\pi]$ cycloaddition of **1** with **2**. Then, the influence of the HB between **2** and water in the cycloaddition was studied through the reaction Model II, in which two water molecules are implicitly included. Solvent effects modeled by a continuum approach over these molecular models have been also considered. Finally, the reaction Model III corresponds to the formal $[2\sigma + 2\sigma + 2\pi]$ cycloaddition of **1** with **8**.

(29) Fukui, K. *J. Phys. Chem.* **1970**, *74*, 4161–4163.
(30) (a) González, C.; Schlegel, H. B. *J. Phys. Chem.* **1990**, *94*, 5523–5527. (b) González, C.; Schlegel, H. B. *J. Chem. Phys.* **1991**, *95*, 5853–5860.
(31) (a) Reed, A. E.; Weinstock, R. B.; Weinhold, F. *J. Chem. Phys.* **1985**, *83*, 735–746. (b) Reed, A. E.; Curtiss, L. A.; Weinhold, F. *Chem. Rev.* **1988**, *88*, 899–926.
(32) Frisch, M. J., et al. *Gaussian 03, Revision C.02*, Gaussian, Inc., Wallingford, CT, 2004.
(33) (a) Tomasi, J.; Persico, M. *Chem. Rev.* **1994**, *94*, 2027–2094. (b) Simkin, B. Y.; Sheikhet, I. *Quantum Chemical and Statistical Theory of Solutions-A Computational Approach*; Ellis Horwood: London, 1995.
(34) (a) Cances, E.; Mennucci, B.; Tomasi, J. *J. Chem. Phys.* **1997**, *107*, 3032–3041. (b) Cossi, M.; Barone, V.; Cammi, R.; Tomasi, J. *Chem. Phys. Lett.* **1996**, *255*, 327–335. (c) Barone, V.; Cossi, M.; Tomasi, J. *J. Comput. Chem.* **1998**, *19*, 404–417.
(35) Parr, R. G.; von Szentpaly, L.; Liu, S. *J. Am. Chem. Soc.* **1999**, *121*, 1922–1924.
(36) (a) Parr, R. G.; Pearson, R. G. *J. Am. Chem. Soc.* **1983**, *105*, 7512–7516. (b) Parr, R. G.; Yang, W. *Density Functional Theory of Atoms and Molecules*; Oxford University Press: New York, 1989.
(37) Kohn, W.; Sham, L. J. *Phys. Rev.* **1965**, *140*, 1133–1138.

Results and Discussion

First, energetic aspects and geometrical parameters of TSs and their electronic structure in terms of bond orders (BO) and natural charges for the reaction Models I and II in the gas phase will be analyzed. Then, the energetic and geometrical results including solvent effects as a continuum model will be discussed. Finally, a DFT analysis based on the reactivity indexes of the reactants involved in these cycloadditions will be performed. The nucleophilic behavior of **1** will be reinforced by study of the reaction Model III.

Study of the Gas-Phase $[2\sigma + 2\sigma + 2\pi]$ Cycloaddition Reaction between 1 and 2, in the Absence and in the Presence of Water Molecules. Reaction Models I and II. An analysis of the stationary points found in the gas-phase cycloaddition reactions between **1** and **2**, in the absence and in presence of two water molecules, indicates that these reactions have a two-stage mechanism. Therefore, two TSs, **TS5** (Model I) and **TS6** (Model II), and two cycloadducts **3** and **6**, were located and characterized (see Scheme 4).

SCHEME 4

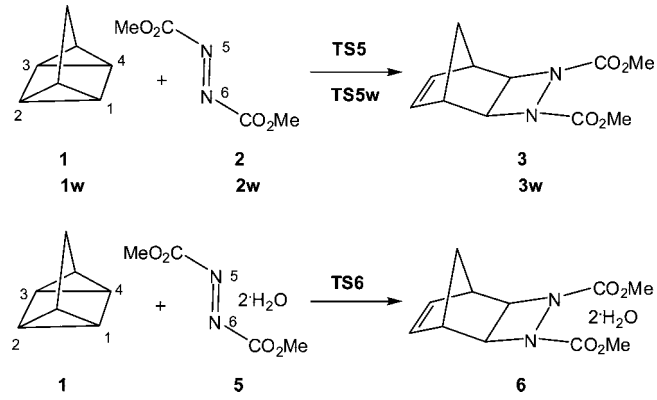

In the gas phase, the MPWB1K/6−31G** activation barrier associated to the cycloaddition reaction between **1** and **2** (Model I) is 23.2 kcal/mol (**TS5**) (see Table 1). With the inclusion of two water molecules hydrogen-bonded to **2** (Model II), the activation barrier of the cycloaddition decreases to 15.1 kcal/mol (**TS6**). Despite B3LYP calculations yield barriers ca. 5 kcal/mol lower than those obtained with MPWB1K, both methods predict a similar acceleration with the HB formation. This acceleration can be related to the increase of the electrophilicity of **5** with the HB formation that favors the cycloaddition through a more polar process (see later). It is worth noting that this acceleration will not be feasible without the participation of QDC **1** as a good nucleophile.[12a] These formal $[2\sigma + 2\sigma + 2\pi]$ cycloadditions are strongly exothermic: −69.8 (**3**) and −77.2 (**6**) kcal/mol. An important part of these energies can be associated to the loss of strain present in the structure of QDC.

The MPWB1K/6−31G** geometries of the TSs are given in Figure 1. Both DFT methods gave similar geometries, the MPWB1K lengths being slightly shorter that the B3LYP ones (see Supporting Information). The lengths of the C−N forming-bonds at the TSs are 1.957 and 2.750 Å at **TS5** and 2.000 and 2.660 Å at **TS6**, while the lengths of the C−C breaking-bonds are 1.776 and 1.519 Å at **TS5** and 1.790 and 1.536 Å at **TS6**. These lengths indicate that these TSs correspond to a highly asynchronous bond-formation processes. The HB influences the TS to be slightly more early. At the hydrogen-bonded **TS6**, the lengths of the HB are 1.887 Å (H−N) and 2.107 Å (H−O),

TABLE 1. Relative (in kcal/mol) Energies, in the Gas Phase, and in Water, of the Stationary Points Involved in the Polar [2σ + 2σ + 2π] Cycloaddition Reaction of 1 with 2, and with 5, Reaction Models I and II

	B3LYP	MPWB1K
	In the Gas Phase	
Model I		
TS5	18.5	23.2
3	−63.1	−69.8
Model II		
TS6	9.9	15.1
6	−70.4	−77.2
	In Water	
Model I		
TS5w	13.6	19.3
3w	−64.4	−71.1
Model II		
TS7w	7.2	14.7
Zw		−29.9
TS8w	−29.1	−29.9
6w	−68.4	−72.9

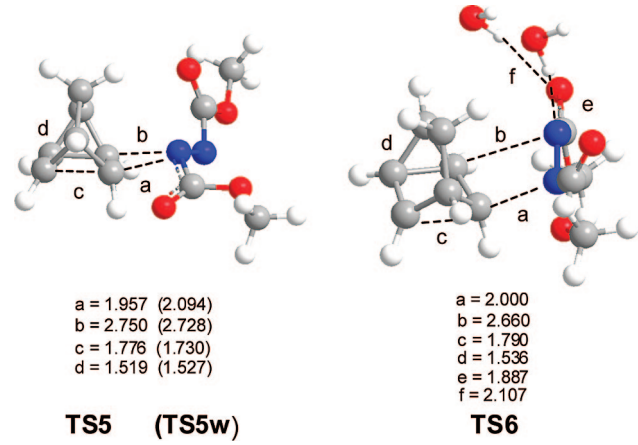

FIGURE 1. MPWB1K/6−31G** transition structures associated with the formal [2σ + 2σ + 2π] cycloaddition reactions of **1** with **2**, and with **5**. The distances are given in angstroms.

while at the reagent **5**, these values are 2.007 Å (H−N) and 2.652 Å (H−O). These values indicate a shortness of the HB lengths at the TS as a consequence of the charge transfer (CT) that takes place along the reaction.[12a,17]

The IRCs from these TSs to cycloadducts show that these cycloadditions have a two-stage mechanism. On going from TS to cycloadduct, the reaction progresses with the formation of the C1−N6 bond, and only when it is completely formed does the C4−N5 bond formation begin. From the IRCs, structures named half-pathway (HP) have the C1−N6 bond that is already formed whereas the C4−N5 bond formation is very delayed.[20,22]

The electronic structure of the TSs associated to these cycloadditions was analyzed using the Wiberg BO[38] and the natural charges obtained by a NBO[31] analysis. The BO values of the C−N forming-bonds at the TSs are 0.41 and 0.04 at **TS5** and 0.39 and 0.05 at **TS6**, while the BO values of the C−C breaking-bonds are 0.54 and 0.90 at **TS5** and 0.52 and 0.86 at **TS6**. These values show the high asynchronicity of the forming- and breaking-bond processes. The more favorable **TS6** is slightly more delayed than **TS5**. At the HPs, the BO values of the C−N forming-bonds are ca. 1.0 and 0.2. At these structures, while the C1−N6 bond is already formed, the C4−N5 bond-formation is very delayed. These results support the nonconcerted character of these two-stage cycloadditons.[20]

The natural population analysis (NPA) allows the evaluation of the CT at these cycloaddition reactions. The MPWB1K/6−31G** natural atomic charges at the TSs were shared between the QDC and the DMAD frameworks. The net charge at the DMAD framework at these TSs is −0.46e at **TS5** and −0.49e at **TS6**. These large values, which are in agreement with the large dipole moment of the TSs (3.43 Debye for **TS5** and 8.32 Debye for **TS6**) point out the large zwitterionic character of these species. The CT is slightly larger at the more early and favorable **TS6**. At the HPs, the CT is −0.77e. During the nucleophilic attack of **1** to **2** or **5** there is an increase of the CT until complete formation of the first C−N bond. With formation of the second C−N bond there is a reduction of the CT as a consequence of a retrodonation process.

At this point, it is interesting to note some differences between the polar two-stage mechanism found by us and the biradical stepwise mechanism proposed by Jung and Marcus for the neat reaction shown in Scheme 3.[23] The UB3LYP/6−31+G* **TS2** has a geometry and electronic structure similar to that of **TS5**. The net charge at the DMAD framework at these TSs is −0.45e at **TS2** (UB3LYP/6−31+G*) and −0.46e at **TS5**, (MPWB1K/6−31G**), in clear agreement whit the high dipole moment of the TSs (3.67 Debye (**TS2**) and 3.43 Debye (**TS5**)). On the other hand, the net charge at the DMAD framework at biradical intermediate **BR3** ($\langle S^2 \rangle = 0.92$), −0.31e, and the dipole moment, 1.29 Debye, are unlike to those found at the HPs of the IRC from **TS5** to **3** at the MPWB1K/6−31G** level, CT = −0.77e and the dipole moment = 6.45 Debye. Therefore, the intermediate **BR3**, which has been associated to a stepwise biradical mechanism, appears to be nonconsistent with the large zwitterionic character of **TS2**. On the other hand, the gas-phase MPWB1K/6−31G** **TS6** has the same geometrical and electronic structure than the B3LYP/6−31+G* **TS4**, and they correspond also to a two-stage mechanism with a large polar character. This fact was confirmed by performing a B3LYP/6−31+G* IRC from **TS4** to cycloadduct. In consequence, the mechanism in the surface reaction via **TS4** is nonconcerted.

Solvent Effects Modeled by the Polarizable Continuum Model. Explicit solvent effects of water were modeled using the PCM method by means of geometrical optimizations of the gas-phase stationary points of reaction Models I and II. The stationary points found in water are given in Schemes 4 and 5, while Table 1 reports the relative energies.

In water, all species associated to the reaction Model I are stabilized between 9 and 15 kcal/mol. The most stabilized species is **TS5w** because of its large zwitterionic character. Consequently, the activation barrier associated to the cycloaddition reaction between **1w** and **2w** is 19.3 kcal/mol. With the inclusion of water as a continuum model, a reduction of 3.9 kcal/mol of the gas-phase barrier is found, in clear agreement with the large polar character of the reaction. Note that this reduction is lower than that observed through the explicit solvation with two water molecules, 8.1 kcal/mol. The reaction is exothermic in −71.1 kcal/mol.

The more noticeable effect with the inclusion of solvent through the PCM is the change of the molecular mechanism for the reaction Model II; a two-step mechanism emerges with the discrete-continuum model (see Scheme 5).[12a] An exhaustive exploration of the MPWB1K/6−31G** potential energy surface for the reaction Model II in water allowed us to find two TSs and one zwitterionic intermediate associated to a two-step

(38) Wiberg, K. B. *Tetrahedron* **1968**, *24*, 1083–1096.

mechanism, **TS7w**, **Zw**, and **TS8w** (see Scheme 5). Both functionals give a very flat surface around **Zw** and **TS8w**; this fact made unfeasible the localization of the corresponding zwitterionic intermediate at the B3LYP/6−31G** level. The first and rate-limiting step corresponds to the nucleophilic attack of **1w** to the water hydrogen-bonded **5w** via **TS7w**, while the second step corresponds to a cyclization process. In water, all species associated to the reaction Model II are stabilized between 14 and 19 kcal/mol. As for the Model I, **TS7w** is largely stabilized as a consequence of its large zwitterionic character (see later). Thus, the activation barrier associated to the cycloaddition reaction between **1w** and **5w** decreases to 14.7 kcal/mol. The intermediate **Zw** is located −29.7 kcal/mol below the reagents. This intermediate with an unappreciable barrier affords the cycloadduct **6w**, via **TS8w**. Formation of this product is exothermic at −72.9 kcal/mol.

SCHEME 5

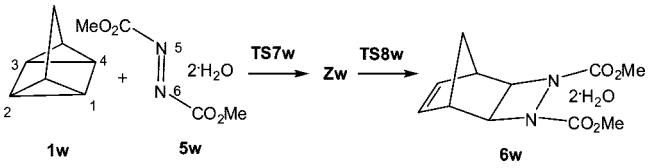

The MPWB1K/6−31G** energy profiles for the [2σ + 2σ + 2π] cycloadditions of **1** with ethylene in the gas phase, profile a, with **2** in the gas phase, profile b, and with **5** in water, profile c, are given in Figure 2. After the implicit and explicit inclusion of water (profile c), the gas-phase energy associated to the nucleophilic attack of **1** to **2**, profile b, is reduced in 8.5 kcal/mol. It is worth noting the large reduction of the gas-phase activation barriers for the polar [2σ + 2σ + 2π] cycloadditions of **1** with **2**, profile b, relative to that for the nonpolar cycloaddition reaction of **1** with ethylene, profile a, 13.2 kcal/mol. Thereby, the large increase of the polar character of the cycloadditions on going from a poor electrophile as ethylene to a good electrophile as DMAD causes a larger reduction of the activation barriers associated to these cycloadditions than that obtained with the implicit inclusion of water. Consequently, the large acceleration experimentally observed "on water" with the increase of the electrophilic character of the solvated DMAD cannot be feasible without the participation of QDC as a good nucleophile in a polar reaction. The profile b also shows the location of the HPs, which share the two-stage mechanism. Note that these points of the IRC from **TS5** to **3** resemble geometrically and energetically the structure **TS8w** of the two-step mechanism given in the profile c.

The MPWB1K/6−31G** geometries of the TSs in water are given in Figures 1 and 3. A comparison of the more relevant geometrical parameters of **TS5** (gas phase) and **TS5w** (in water) given in Figure 1 indicates that there are no noticeable changes with the inclusion of water as a continuum model. While at **TS5w** the length of the C1−N6 forming-bond increases slightly to 2.094 Å, the length of the C1−N6 breaking-bond decreases to 1.730 Å. These changes point to the earlier character of **TS5w** in water.

At the two-step mechanism, the length of the C1−N6 forming-bond at **TS7w** is 2.088 Å, while the distance between the C4 and N5 centers is 2.745 Å. At this TS, the lengths of the C1−C2 and C3−C4 σ breaking-bonds are 1.749 and 1.539 Å, respectively. The lengths of the HBs at **TS7w** are 1.946 and 1.978 Å. These geometrical parameters are very similar to those

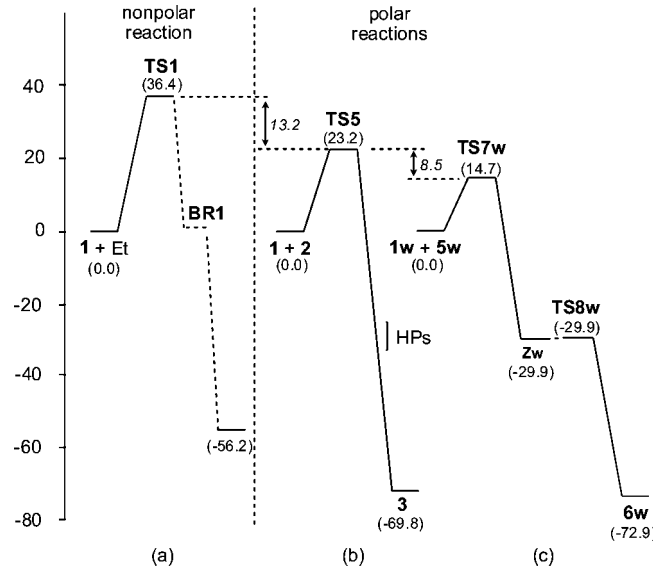

FIGURE 2. MPWB1K/6−31G** energy profiles for the [2σ + 2σ + 2π] cycloadditions of **1** with (a) ethylene (in the gas phase), (b) **2** (reaction Model I in the gas phase) and (c) **5w** (reaction Model II in water). In parentheses relative energies in kcal/mol.

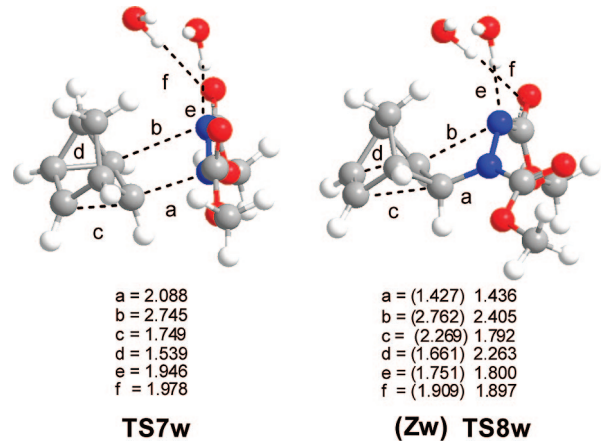

FIGURE 3. MPWB1K/6−31G** transition structures associated with the stepwise [2σ + 2σ + 2π] cycloaddition reaction of **1** with **5w**. The distances are given in angstroms.

found at the gas-phase TSs of the Models I and II. At the intermediate **Zw**, the length of the C1−N6 bond is 1.427 Å, while the distance between the C4 and N5 centers remains 2.762 Å. Finally, at **TS8w**, the length of C1−N6 σ bond is 1.436 Å, while the length of the C4−N5 forming-bond is 2.405 Å. The geometry of **TS8w** resembles that of the HPs obtained from the IRC from **TS5w** to cycloadduct **3w**.

The BO values of the C−N forming-bonds at **TS5w** are 0.32 and 0.04, while the BO values of the C−C breaking-bonds are 0.59 and 0.88. These values indicate that **TS5w** is slightly earlier than **TS5**. The BO value of the C1−N6 forming-bond at **TS7w** is 0.33, while the BO value between the C4 and N5 atoms is 0.05. At this TS, the BO values of the C1−C2 and C3−C4 σ breaking-bonds are 0.55 and 0.86. At the intermediate **Zw**, the C1−N6 BO value, 0.97, indicates that this bond is already formed, while the BO value between the C4 and N5 centers remains 0.02. Finally, at **TS8w** the BO value of the C4−N5 forming-bond is 0.12.

In water, the net charge at the DMAD framework of **TS5w** is −0.48e, a value slightly higher than that at gas-phase **TS5**.

TABLE 2. MPWB1K/6-31G Relative (Δ*H* and Δ*G* in kcal/mol) Enthalpies and Free Energies, And Relative (Δ*S*, cal/mol·K) Entropies, Computed at 25 °C and 1 atm, of the Stationary Points Involved in the Polar [2σ + 2σ + 2π] Cycloaddition Reaction of QDC 1 with DMAD 2, Models I (in the gas phase) and II (in water)**

	Δ*H*	Δ*S*	Δ*G*
Model I: in the gas phase			
TS5	23.2	−50.1	38.2
3	−65.9	−54.3	−49.7
Model II: in water			
TS7w	15.6	−46.7	29.6
Zw	−26.9	−46.4	−13.1
TS8w	−27.5	−51.8	−12.0
6w	−68.8	−57.7	−51.6

This increase of the CT is in agreement with the large dipole moment of **TS5w**, 5.67 Debye. In the two-step mechanism, the net charges at the DMAD framework are: −0.53e at **TS7w**, −1.10e at **Zw**, and −1.05e at **TS8w**. The NPA analysis at the two-step mechanism indicates that there is an increase of the CT along the nucleophilic attack of **1** to **2** until the formation of the zwitterionic intermediate **Zw**. After **TS8w** there is a retrodonation process until the formation of the final cycloadduct **6w**. These results are similar to those obtained from the analysis of the CT along the IRC from **TS6** to cycloadduct **6** in the gas-phase reaction of **1** with **5**.

Finally, thermodynamic calculations were performed at the reaction Model I, in the gas phase, and at the reaction Model II, in water, in order to analyze the effects of thermal corrections and entropies on the relative free energies of the [2σ + 2σ + 2π] cycloaddition of **1** with **2** in water. The relative enthalpies, entropies, and free energies are given in Table 2.

Inclusion of the thermal corrections to the energies raises the activation enthalpies to 23.2 (**TS5**, Model I) and 15.6 (**TS7w**, Model II) kcal/mol. Therefore, **TS7w** remains 7.6 kcal/mol below **TS5**. The inclusion of the activation entropies to the enthalpies raises the activation free energies to 38.2 (**TS5**) and 29.6 (**TS7w**) kcal/mol, as a consequence of the large negative activation entropy associated to these bimolecular processes. Despite this fact, **TS7w** remains 8.6 kcal/mol below **TS5**, a value closer to that obtained from the potential energies, 8.5 kcal/mol. It is worth noting that the computed activation enthalpy for the [2σ + 2σ + 2π] cycloaddition of **1** with **2** in water, 15.6 kcal/mol, is 3.6 kcal/mol higher than the activation energy experimentally reported by Sharpless for the heterogeneous reaction "on water". These results are in reasonable agreement with the faster reaction observed "on water" than in the homogeneous reaction in water.[6] Formation of the zwitterionic intermediate **Zw** and the final cycloadducts **3** and **6w** are strongly exergonic (see Table 2). With the inclusion of the thermal corrections and entropies, **Zw** is 0.9 kcal/mol lower in the free energy surface than **TS8w**. Thus, at the free energy surface, **Zw** is a minimum. Note that at the potential energy surface, **Zw** and **TS8w** are isoenergetic (see Table 1).

We can conclude that the two reaction models (Model I and Model II) correspond to the same polar reactivity pattern associated to the nucleophilic attack of QDC to DMAD. The large nucleophilic character of QDC (see later) together with the large electrophilic character of DMAD accounts for the large reduction of the activation barrier for these cycloadditions compared with the nonpolar reaction between QDC and ethylene via the biradical mechanism. HB formation with two water molecules increases the electrophilicity DMAD. This fact causes a reduction of the activation barrier through a more polar process.[10] This behavior is enhanced when the solvent effect of water is considered through PCM calculations.

TABLE 3. Electronic Chemical Potential, μ in au, Chemical Hardness, η in au, Global Electrophilicity, ω in eV, and Nucleophilicity, N in eV, Values of 1, 2, and 5

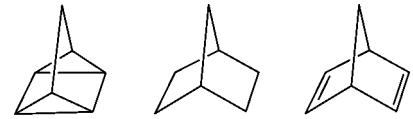

1 **7** **10**

	μ	η	ω	N
DMAD·2H_2O **5**	−0.1809	0.1431	3.11	2.25
DCE **8**	−0.2075	0.2075	2.82	0.65
DMAD **2**	−0.1726	0.1681	2.41	2.14
DMAcD	−0.1816	0.1984	2.26	1.48
10	−0.1084	0.2172	0.74	3.22
ethylene	−0.1239	0.2855	0.73	1.86
7	−0.1025	0.3634	0.39	1.39
QDC **1**	−0.0594	0.3141	0.15	3.23

Analysis Based in the Reactivity Indexes. Recent studies carried out on cycloaddition reactions have shown that the analysis of the reactivity indexes defined within the conceptual DFT[39] is a powerful tool to establish the polar character of the reactions.[10] Recently, we proposed a simple index for the nucleophilicity, N, based on the HOMO energy.[24] The N index has been useful to explain the nucleophilic reactivity of a series of captodative ethylenes toward electrophiles in polar cycloaddition reactions.[24] In Table 3, the static global properties as electronic chemical potential, μ, chemical hardness, η, global electrophilicity, ω, and global nucleophilicity, *N*, for QDC, DMAD, and the complex **5** are presented.

The electronic chemical potential of **1**, −0.0594 eV, is higher than that for **2** and **5**, −0.1726 and −0.1809 au, indicating thereby that along a polar process the net CT will take place from **1** to **2**, in clear agreement with the CT found at the TSs.

The electrophilicity of **2** is 2.41 eV, so it could be classified as a strong electrophile within the electrophilicity scale.[10] Explicit solvation of **2** with two hydrogen-bonded water molecules enhances the electrophilicity of **5** to 3.11 eV. Therefore, it is expected an acceleration of the cycloadditions of **2** in water through an increase of the polar character of the reaction.[12a] **1** presents a very low electrophilicity value, ω = 0.15 eV. This very low value, that is slightly lower than that for bicyclo[2.2.1]heptane,**7**, is a consequence of the saturated nature of these hydrocarbons, and points out the nonparticipation of these hydrocarbons as electrophiles in polar reactions.

In the fifth column of Table 3, the nucleophilicity indexes *N* for these molecules are given. We note the high nucleophilicity value found at QDC, N = 3.23 eV. This nucleophilicity value is slightly higher than that found for methyl vinyl ether, N = 3.20 eV,[24] an electron-rich ethylene that acts as good nucleophile in polar cycloaddition reactions.[9] On the other hand, this value is higher than that computed for **7**, N = 1.39 eV, which is also inert as a nucleophile in polar reactions. These results, which are in clear agreement with the lower ionization potential experimentally obtained for **1** (7.97 ± 0.05 eV) than that for **7** (8.45 ± 0.05 eV),[40] account for the large nucleophilic character of **1** and its participation in polar cycloaddition reactions. The

(39) (a) Geerlings, P.; De Proft, F.; Langenaeker, W. *Chem. Rev.* **2003**, *103*, 1793–1873. (b) Ess, D. H.; Jones, G. O.; Houk, K. N. *Adv. Synth. Catal.* **2006**, *348*, 2337–2361.

(40) Schwell, M.; Dulieu, F.; Gee, C.; Jochims, H. W.; Chotin, J. L.; Baumgartel, H.; Leach, S. *Chem. Phys.* **2000**, *260*, 261–279.

nucleophilic character of **1** can be explained by a stabilization of the positive charge that is developing on the C2 center along the nucleophilic attack of **1** on an electrophilic π molecule by the near strained cyclopropyl moiety that remains on QDC (see Chart 1).

CHART 1

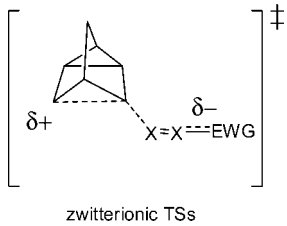

zwitterionic TSs

Study of the Polar Cycloaddition Reactions of 1 and 10 with 8. Reaction Model III. In order to reinforce the study of the polar character of the cycloadditions of QDC with electrophilically activated π molecules, the cycloadditions of **1** and bicyclo[2.2.1]hepta-2,5-diene **10**, a structural isomer alkene of **1**, with DCE **8**, a good electrophilic ethylene,[24] were studied (see Scheme 6). Note that both cycloadditions afford the same formal [2 + 2] cycloadduct **9**. Analysis of the IRC from the unique highly asynchronous TS found at these cycloadditions to **8** indicates that they have also two-stage mechanisms. The geometries of the TSs are given in Figure 4.

SCHEME 6

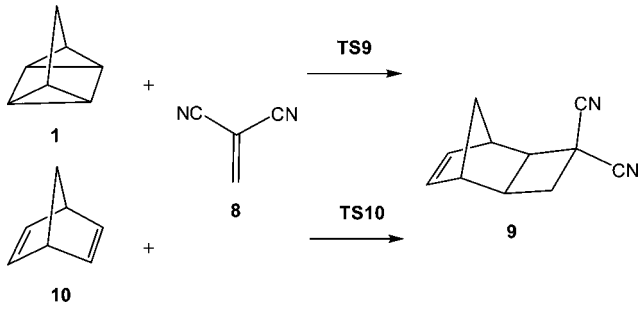

In the gas phase, both cycloadditions present similar activation barriers: 19.4 kcal/mol for the formal [$2\sigma + 2\sigma + 2\pi$] cycloaddition of **1** with **8** via **TS9**, and 20.6 kcal/mol for the formal [2 + 2] cycloaddition of **10** with **8** via **TS10** (see Table 4). The lower activation barrier of the reaction of **8** with **1** than that with **10** is in agreement with the nucleophilic power of the two reagents: $N = 3.23$ eV for **1** and 3.22 eV for **10** (see Table 3). In addition, these activation barriers are lower than that computed for the formal [$2\sigma + 2\sigma + 2\pi$] cycloaddition of **1** with **2**, 23.2 kcal/mol, as a consequence of the larger electrophilic character of DCE, $\omega = 2.82$ eV, than DMAD, $\omega = 2.41$ eV (see Table 3). Inclusion of solvent effects of water by PCM single point calculations for the gas-phase structures reduces the activation barrier to 12.2 kcal/mol at **TS9** and 13.1 kcal/mol at **TS10**, as a consequence of the large polar character of these species. These energy results are in complete agreement with the large dipole moments of the TSs: 9.03 Debye at **TS9** and 7.44 Debye at **TS10**, and with the CT computed at both TSs. The charge of the DCE framework at both TSs is −0.33e. These data point to the large polar character of these cycloadditions.

Finally, the geometries of the TSs are given in Figure 4. Note that the lengths of the forming- and breaking-bonds at **TS9** are

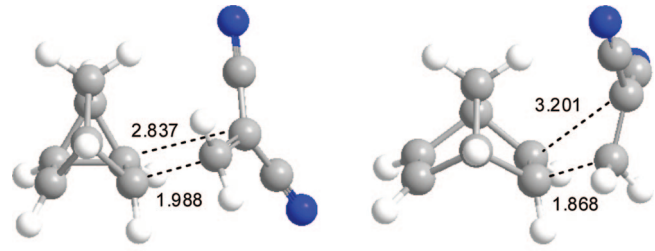

FIGURE 4. MPWB1K/6−31G** transition structures associated with the formal cycloaddition reactions of **1** and **10** with **8**. The distances are given in angstoms.

TABLE 4. MPWB1K/6-31G Relative Energies (ΔE in kcal/mol), in the Gas Phase and in Water, of the Stationary Points Involved in the Polar Cycloaddition Reactions of 1 and 10 with 8**

	in the gas phase	in water
TS9	19.4	12.2
TS10	20.6	13.1
9	−54.6	−53.8

similar to those found at the TS associated to the formal [$2\sigma + 2\sigma + 2\pi$] cycloaddition of **1** with **2** via **TS5** (see Figure 1). These results, which are similar to those obtained for the reaction Models I and II, point out the participation of QDC as a good nucleophile in polar cycloadditions toward electrophilically activated π molecules as DMAD and DCE.

Conclusions

The formal [$2\sigma + 2\sigma + 2\pi$] cycloaddition reaction of quadricyclane **1** with dimethyl azodicarboxylate **2** in water has been studied using DFT methods. Solvent effects of water have been modeled by means of a discrete-continuum model. In the gas phase, formation of specific HBs between two water molecules and **2** decreases the activation barrier from 23.2 to 15.1 kcal/mol. Inclusion of solvent effects through the combination of discrete and polarizable continuum models changes the mechanism from a two-stage to a two-step mechanism. In all cases, the reaction is initialized by the nucleophilic attack of **1** to one electrophilic activated nitrogen of **2**. With the inclusion of water by means of a discrete-continuum model, a large reduction of the gas-phase activation barrier is observed as a consequence of the increase of the polar character of the cycloaddition and the stabilization of the corresponding zwitterionic TS. The computed activation enthalpy for the discrete-continuum model of the [$2\sigma + 2\sigma + 2\pi$] cycloaddition of **1** with **2** in water, 15.6 kcal/mol, is in reasonable agreement with experimental outcome.[6]

An analysis of the global electrophilicity and nucleophilicity of the reagents provides a sound explanation about the participation of quadricyclane **1** as a strong nucleophile in polar cycloadditions. While the increase of electrophilicity of **2** with the HB formation accounts for the increase of the polarity of the process, the large nucleophilic character of **1** accounts for the participation of this strained hydrocarbon in a polar process. A further comparative study of the cycloadditions of **1** with 1,1-dicyanoethylene **8**, a good electrophilic ethylene, allows us to assert the polar character of these cycloadditions as a consequence of the nucleophilic behavior of **1**. We can conclude that the large acceleration found for Sharpless for the reaction of **1** with **2** "on water"

would not be feasible without the large nucleophilic character of quadricyclane, which allows its participation in the polar cycloadditions toward electrophilic π molecules. Finally, the large reduction of the activation enthalpy found in water by the hydrogen-bond formation indicates that it plays a relevant role in the large acceleration experimentally observed by Sharpless in the reaction "on water".

Acknowledgment. This work was supported by research funds provided by the Ministerio de Ciencia e Innovación of the Spanish Government (project CTQ2006-14297/BQU).

Supporting Information Available: Complete citation for ref 32 B3LYP/6−31G** and MPWB1K/6−31G** total energies, in the gas phase and in water, of the stationary points of the reaction Models I−III. MPWB1K/6−31G** total enthalpies, entropies, and free energies of the stationary points of the reaction Model I in the gas phase and Model II in water. B3LYP/6−31G** geometries and MPWB1K /6−31G** Cartesian coordinates of the TSs and intermediate **Zw**. This material is available free of charge via the Internet at http://pubs.acs.org.

JO801575G